NASA TECHNICAL NOTE

NASA TN D-4192

NASA TN D-4192

EXPERIMENTAL INVESTIGATION OF THE EFFECT OF MODEL SCALE ON STRUCTURAL-JOINT DAMPING

by David G. Stephens, Brantley R. Hanks, and Maurice A. Scavullo

Langley Research Center
Langley Station, Hampton, Va.

NATIONAL AERONAUTICS AND SPACE ADMINISTRATION • WASHINGTON, D. C. • OCTOBER 1967

NASA TN D-4192

EXPERIMENTAL INVESTIGATION OF THE EFFECT OF MODEL SCALE ON STRUCTURAL-JOINT DAMPING

By David G. Stephens, Brantley R. Hanks, and Maurice A. Scavullo

Langley Research Center
Langley Station, Hampton, Va.

NATIONAL AERONAUTICS AND SPACE ADMINISTRATION

For sale by the Clearinghouse for Federal Scientific and Technical Information
Springfield, Virginia 22151 – CFSTI price $3.00

EXPERIMENTAL INVESTIGATION OF THE EFFECT OF MODEL SCALE ON STRUCTURAL-JOINT DAMPING

By David G. Stephens, Brantley R. Hanks, and Maurice A. Scavullo
Langley Research Center

SUMMARY

An investigation was conducted to determine the effect of model scale or size on structural-joint damping. A cantilever configuration was utilized wherein the beam was bolted between two angle brackets at the support. Four geometrically similar assemblies, covering a scale range of approximately 20 to 1, were tested. Free decay of the fundamental mode was measured over a range of joint clamping pressures and beam-tip amplitudes. Also, damping resulting from the addition of liquid lubricants or plastic films to the joint interfaces was investigated. Data indicate that a decrease in model size results in an increase in the damping attributed to the structural joint. Furthermore, the magnitude of the joint damping is slightly dependent on vibration amplitude and is an inverse function of joint clamping pressure. Structural-joint damping may be substantially increased by the addition of liquid lubricants or plastic films to the joint interfaces.

INTRODUCTION

Dynamic models are often used to study the vibratory response of complex systems when full-scale testing is precluded by system size and/or cost. A prerequisite for model testing is a knowledge of the proper scaling relationships required to extrapolate model data to the full-scale systems. A considerable amount of information has been obtained on the scaling relationships for frequencies and mode shapes. However, the variation of damping with model size or scale is largely unknown and often either neglected or considered to be the same in both model and prototype. The development of proper scaling relationships for damping requires a knowledge of each of the damping mechanisms in the system, such as material hysteresis (e.g., refs. 1 and 2), air damping (e.g., refs. 3 and 4), and joint damping (e.g., refs. 5 to 10). In space systems, scaling relationships for joint damping are of particular importance since the major source of energy dissipation in such systems is usually attributed to structural interfaces or joints (ref. 5).

Joint damping has been studied both experimentally and analytically for a variety of joint configurations. For example, Ungar (ref. 6) examined several types of joints used in fastening and bracing plates. Air pumping caused by normal motions of the mating surfaces was concluded to be the primary energy-dissipation mechanism in joints having some flexibility; however, interfacial slip was also a contributing factor in relatively stiff joints. Goodman and Klumpp (ref. 7) examined, theoretically and experimentally, the damping of a longitudinally split cantilever beam clamped under uniform pressure. Assuming a Coulomb friction-force boundary condition at the interface and utilizing specially prepared interface surfaces which had Coulomb friction characteristics, good experimental and analytical agreement was obtained. Pian and Hallowell (ref. 8) investigated the energy losses due to bending of simple built-up beams (i.e., beams having thin plates joined to the top and bottom with screws). Their analysis assumed that the screws supported no shear load and that sliding friction was the damping mechanism. The analytical solution obtained agreed well with experimental static-hysteresis data. In an extension of this work, Pian (ref. 9) showed that screws which do support a shear load can be analyzed as a continuous shear joint. Mentel (ref. 10) examined theoretically the damping of beams built into rigid structures at the supports. Damping due to viscoelastic inserts at the supports as well as Coulomb friction was considered. Limited experimental results were presented which showed damping to be considerably higher than predicted. This added damping was attributed to rotational motion at the supports whereas only motion along the longitudinal axis of the beam was considered in the theory.

Although it has not been verified experimentally, the theoretical joint-damping expressions developed by the above investigators indicate that the energy loss per cycle varies as the cube of the scale factor. Since the total energy of the beam (at a given nondimensional vibration amplitude) also varies as the scale factor cubed, the logarithmic decrement, which is the ratio of energy loss per cycle to twice the total energy, is predicted to be independent of scale factor.

The purpose of the investigation reported herein was to determine experimentally the effect of model scale on joint damping for a range of interface and vibratory conditions. The joint damping of four cantilever systems, covering a geometric scale range of 20 to 1, was examined. Data are presented to show the effect of vibration amplitude, joint clamping pressure, and model scale, as well as the effect of interface lubricants and plastic films, on the magnitude of the damping in structural joints.

SYMBOLS

Measurements for this investigation were taken in the U.S. Customary Units. Equivalent values in the International System of Units (SI) are indicated herein in the

interest of promoting the use of this system. The conversion factors required for units used in the present study are presented in appendix A.

A	joint interface area, in^2 (m^2)
c	specific heat per unit volume, $\frac{\text{in-lb}}{\text{in}^3\text{-}^\circ\text{R}}$ $\left(\frac{\text{m-N}}{\text{m}^3\text{-}^\circ\text{K}}\right)$
D	bolt diameter, in. (m)
E	modulus of elasticity, lb/in^2 (N/m^2)
F	clamping force per bolt, lb (N)
f	frequency of vibration, cps (Hz)
k	thermal conductivity, $\frac{\text{in-lb}}{\text{in-sec-}^\circ\text{R}}$ $\left(\frac{\text{m-N}}{\text{m-sec-}^\circ\text{K}}\right)$
M	bolt torque, in-lb (m-N)
N	number of cycles
P	interface clamping pressure, lb/in^2 (N/m^2)
p	chamber pressure, torr (N/m^2)
T	absolute temperature, $^\circ R$ ($^\circ K$)
t	beam thickness, in. (m)
y	vibratory displacement amplitude, in. (m)
α	thermal coefficient of linear expansion, $1/^\circ R$ ($1/^\circ K$)
δ	logarithmic decrement of damped oscillation, $\frac{1}{N} \log_e \frac{y_n}{y_{n+N}}$
λ	scale factor
μ	oil viscosity, cP ($N\text{-sec}/m^2$)

τ relaxation time for temperature equalization, sec

ω circular frequency, rad/sec

Subscripts:

j joint

m material

n nth cycle of vibration

APPARATUS AND TEST PROCEDURE

The apparatus used in this investigation is shown in figures 1 and 2. It consisted of four geometrically scaled beams bolted between correspondingly scaled angle brackets. The angle brackets were, in turn, clamped to a massive concrete and steel supporting block, as shown in sketch (a). The four models had scale factors λ of 1, 0.667, 0.333,

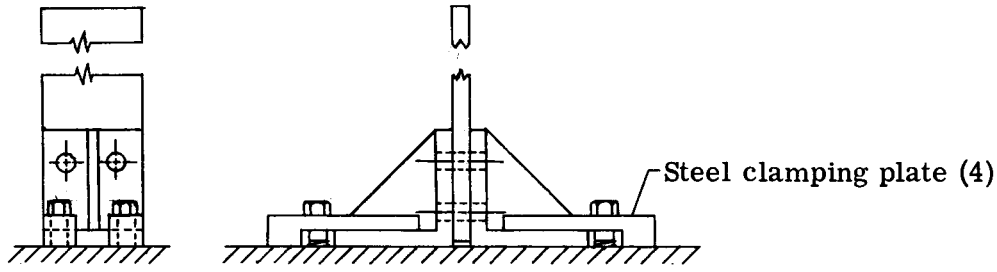

Sketch (a)

and 0.053 with the beams ranging from 60.1 inches (152.65 cm) down to 3.2 inches (8.13 cm) in overall length. The beams and angle brackets were made of 6061 aluminum alloy with all surfaces finished to 63 microinches (0.0016 mm) rms. Each angle bracket was machined from a single piece of aluminum and had a center web to provide rigidity.

Three joint interface conditions (dry, oil-coated, and plastic-film-insert) were studied in an effort to find a method for increasing the inherent joint damping of both small- and large-scale systems. The effect of dry and oil-coated joint conditions was studied on all four models whereas the effect of plastic-film inserts was studied on the 0.667-scale model only. In studying the effect of joint lubrication, the interfaces were coated with a thin layer of oil before assembly. Oil viscosities of 150, 525, and 1400 centipoises were utilized. The effect of plastic-film inserts was studied using

three film materials – 0.5-mil-thick (0.0127-mm) teflon, 0.5-mil-thick (0.0127-mm) polyethylene terephthalate, and 1.0-mil-thick (0.0254-mm) polypropylene. The films were cut to the shape of the joint interface and placed in position during model assembly.

The test procedure was essentially the same in all cases. The total damping of the system was measured at atmospheric pressure for a range of joint clamping pressures (by varying bolt tightening torque) and beam-tip amplitudes. For a particular clamping pressure, the beam was deflected manually and released to oscillate in the first cantilever vibration mode. Oscillations of the beam were sensed by an electrical strain gage attached to one side of the beam as shown in figure 1. The strain gage was coupled, through an amplifier, to an electronic damping meter, which is a device for determining the frequency and damping of a vibrating system. Basically, the damping meter counted the number of cycles as the amplitude decayed between preset limits. The logarithmic decrement δ was then calculated from the equation

$$\delta = \frac{1}{N} \log_e \frac{y_n}{y_{n+N}}$$

where N was the number of cycles counted, y_n was the amplitude at which counting started, and y_{n+N} was the amplitude at which counting ceased. In all tests, the ratio of start amplitude to stop amplitude was maintained at 10/7 so that

$$\delta = \frac{1}{N} \log_e \frac{10}{7}$$

Since the damping was measured over a band (y_n, y_{n+N}) of the decay envelope, the logarithmic decrement was specified at the average amplitude of this band. Measurements were made at several amplitude levels for each bolt torque by varying the triggering voltage of the damping meter. In all tests, sufficient initial deflection was given to the beam to allow transients to die out before the triggering amplitude of the damping meter was reached. Each test was repeated at least five times and the average value of the data was used. The data were repeatable within 5 percent for each test series and within 10 percent after dismantling and reassembling of the models.

The clamping force exerted by each bolt was calculated using the relationship (ref. 11)

$$F = \frac{M}{0.2D}$$

where F is the clamping force per bolt, M is the torque, and D is the nominal bolt diameter. The average clamping pressure produced by the four bolts is, therefore,

$$P = 20 \frac{M}{DA}$$

where P is the average clamping pressure and A is the joint interface area. No allowance was made for variation of clamping pressure across the interface.

MATERIAL AND AIR DAMPING CONSIDERATION

The determination of the magnitude of joint damping in a complex system involves the separation of the total damping into its various components. One contribution to the total damping is that of hysteresis within the material comprising the system. Experimental separation and measurement of material hysteresis damping is difficult in systems such as the one under study; however, an analytical expression developed by Zener (ref. 1) has been experimentally verified for aluminum in reference 2. Material damping in a cantilever beam was shown to be closely approximated by the equation

$$\delta_m = \frac{\pi \alpha^2 E T}{c} \left(\frac{\omega \tau}{1 + \omega^2 \tau^2} \right)$$

where, for a flat beam of uniform thickness, $\tau = \frac{t^2 c}{\pi^2 k}$. The material damping as predicted by this equation is shown as a function of frequency in figure 3(a) for the beams used in this study. The magnitude of the material damping at the fundamental resonant frequency is presented as a function of scale factor in figure 3(b). For the systems under study, material damping as predicted by the Zener equation is essentially inversely proportional to scale.

In considering the air damping, there is virtually no information available which is directly applicable to the configurations under study. However, based on the results of references 3 and 4, which considered systems with much higher ratios of surface area to mass as well as higher vibration amplitudes than those encountered in the present tests, the air damping is estimated to be a small percentage of the total measured damping. This conjecture was verified in limited tests conducted with the 0.053-scale model at a chamber pressure p of 0.2 torr (26.7 N/m^2). The air damping was found to be at least one order of magnitude less than the total damping of the model.

RESULTS AND DISCUSSION

The test program consisted of an isolation and examination of the damping for the following variables: vibratory amplitude, joint clamping pressure, model scale, and interface condition (i.e., dry, lubricated, or plastic-film insert). The dependency of the

damping on each of these variables is illustrated by representative data in the following sections.

As previously noted, the vibratory frequency was measured simultaneously along with each damping measurement. The nominal values of frequency recorded were 11.3, 16.9, 33.6, and 218.0 Hz for the $\lambda = 1$, $\lambda = 0.667$, $\lambda = 0.333$, and $\lambda = 0.053$ models, respectively. It is interesting to compare the measured values with those calculated from classical beam theory. Based on the length of each beam extending beyond the angle bracket (dimension A minus dimension C, see fig. 2), the calculated values are 11.4, 17.0, 34.1, and 214.5 Hz, which are in good agreement with the measured values. There was no apparent or consistent variation in frequency with vibratory amplitude or clamping pressure, the observed deviations being less than 1 percent of the nominal values.

Dry Interface

Effect of vibration amplitude.- The damping measured for each model is shown in figure 4. The total damping in terms of the logarithmic decrement δ is presented as a function of the ratio of vibratory displacement amplitude to beam thickness y/t for four or more values of joint clamping pressure. For the range of amplitude investigated, the total damping exhibits an approximately linear increase with an increase in amplitude ratio for all models. Since the total damping represents not only losses in the joints but also internal hysteresis and air damping, a closer inspection of the data is needed to determine whether the joint damping per se is amplitude dependent. The slopes of the faired lines in figure 4 are observed to increase with a decrease in clamping pressure (a variable affecting joint damping only). This fact suggests that the joint damping increases linearly with increasing amplitude.

Effect of joint clamping pressure.- The total damping for each of the models is presented as a function of joint clamping pressure in figure 5. These curves are simply cross plots of the damping-amplitude curves of figure 4. For all models, the total damping decreases with increasing clamping pressure. This decrease is pronounced in the low-pressure range while at higher clamping pressures the damping appears to approach a constant value asymptotically. It is assumed that a change in clamping pressure has no effect on the extraneous sources of damping, such as hysteresis, air damping, and interface damping between the angle bracket and the base support. Therefore, the increment in damping over and above the asymptotic value must emanate in the joint itself. It is further assumed that the joint damping is negligible at high clamping pressure (see ref. 1, for example) and thus the damping below the asymptote is extraneous and can be considered as tare damping. The magnitude of the joint damping at a particular pressure and amplitude is determined by subtracting the respective high clamping stress asymptote or tare from the measured total damping of figure 5. This technique

was used to obtain the values of joint damping to be presented and discussed in the following sections. It should be pointed out that this method involves taking the difference between two relatively large numbers and therefore the resultant joint damping is quite sensitive to the fairing in figure 5. The sensitivity, however, is not so critical as to affect the trends of the data and conclusions which follow.

Effect of scale.- The variation of total damping with scale factor is shown in figure 6 for two values of the joint clamping pressure. All the data between the amplitude-ratio limits (y/t of 0.03 to 0.08) fall within the indicated band. These data demonstrate that total damping increases with decreasing scale factor and is substantially higher for the smaller models. The trends of these curves are very similar to the Zener relationship for the variation of material damping with scale factor.

The damping δ_j attributed to the structural joint is presented as a function of scale factor in figure 7. The values presented were obtained by subtracting the tare damping (the damping at high clamping stress (fig. 5)) from the total damping measured at lower stress levels. Data shown for all four beams in figure 7(a) demonstrate that joint damping is an inverse function of the scale factor. In order to illustrate this trend more clearly for the larger models, the data for the three larger beams are repeated in figure 7(b) on a magnified damping scale. For the range of scale factors considered, the joint damping is reduced by two orders of magnitude in going from the smallest ($\lambda = 0.053$) to the largest ($\lambda = 1$) model. Thus, caution should be used in extrapolating damping data obtained in tests of small models to full-scale systems, especially when a number of structural joints are involved. The practice of assuming that the damping of the prototype is the same as in the model could lead to gross overestimates of the damping in full-scale systems.

The variation of joint damping with scale factor as found in these tests is not predicted by available theory (refs. 7 and 9, for example). For a given beam, however, there is qualitative agreement between theory and experiment in that joint damping decreases with increasing clamping pressure and is not highly dependent upon the amplitude of vibration. In the reference studies where good experimental and theoretical correlation was obtained, sliding friction forces were usually determined in separate tests and the measured values were used in the theoretical prediction. This suggests that the friction forces as well as the magnitude of interfacial slip may be dependent upon scale and/or frequency although this dependency is not included explicitly in the analyses.

Treated Interfaces

Effect of oil.- In an effort to alter the joint damping, the effects of interface lubricants were examined. Typical results are shown in figure 8 where the total damping for each of the four models, with oil ($\mu = 150$ cP) added to the joint interfaces, is presented

as a function of amplitude. As in the dry joint condition, the total measured damping varies linearly with amplitude. Changing the joint clamping pressure produces a change in slope of the curves which suggests that the joint damping also varies linearly with amplitude within the amplitude range covered.

The same data are presented in figure 9 to show the effect of joint clamping pressure on the damping of each model. The effect of clamping pressure on damping is essentially the same in both the lubricated and the dry condition; however, the addition of oil to the joint interfaces significantly increases the magnitudes of the damping in all but the smallest model where the addition of oil slightly decreased the damping. Similar tests were performed by Klint and Owens (ref. 12) wherein the effect on damping of adding grease to the root of a cantilever was studied. The grease was shown to increase the damping by a factor of approximately two.

The variation of total damping with lubricant viscosity is exemplified in figure 10 for the 0.667-scale model. Increasing viscosity by about one order of magnitude is shown to have a relatively small effect on the damping.

Effect of plastic-film inserts.- The effect of adding plastic-film inserts to the joint interfaces of the 0.667-scale model is summarized in figure 11. Figure 11(a) shows the variation of total damping with joint clamping pressure for three different insert materials. The trends of the data are essentially the same as those for the dry and lubricated joint conditions. In figure 11(b), the range of total damping obtained with each film material is compared with the ranges for the lubricated and dry joint conditions. The film materials are shown to increase the damping substantially, although they are not significantly more effective than oil in this respect.

The use of plastic films and liquid lubricants undoubtedly reduces the coefficient of friction in the joints. The increased energy dissipation, therefore, must result from a combination of the viscoelastic shearing in the constrained layer (ref. 13) as well as increased interfacial slip and oil pumping. Considerable additional experiments are required to define these mechanisms explicitly. The significant increase in damping demonstrated by these tests, however, indicates the excellent potential of joint treatments for increasing structural damping.

CONCLUSIONS

An investigation was conducted to determine the effect of model scale or size on structural-joint damping. In addition, the effect of adding lubricants or plastic films to the joint interfaces was studied. The following conclusions were obtained:

1. The magnitude of the damping attributed to the structural joint exhibits a small linear increase with an increase in vibration amplitude.

2. Joint damping decreases with increasing joint clamping pressure.

3. Both the total damping of the assembly and the joint damping increase appreciably with a reduction in model scale or size.

4. The addition of liquid lubricants or plastic films to the joint interfaces can substantially increase the structural-joint damping.

Langley Research Center,
National Aeronautics and Space Administration,
Langley Station, Hampton, Va., April 11, 1967,
124-08-05-01-23.

APPENDIX A

CONVERSION OF U.S. CUSTOMARY UNITS TO SI UNITS

Factors required for converting the U.S. Customary Units used herein to the International System of Units (SI) are given in the following table:

Physical quantity	U.S. Customary Unit	Conversion factor (*)	SI Unit
Area	inches^2 (in^2)	6.4516×10^{-4}	meters (m^2)
Force	pounds (lb)	4.4482	newtons (N)
Frequency	cycles per second (cps)	1	hertz (Hz)
Length	inches (in.)	2.54×10^{-2}	meters (m)
	mils	2.54×10^{-5}	
	microinches (μin.)	2.54×10^{-8}	
Pressure, Modulus	lb/in^2 = psi	6.8947×10^3	newtons/meter^2 (N/m^2)
	torr	1.3332×10^2	
Specific heat	$\frac{\text{in-lb}}{\text{in}^3\text{-}^\circ\text{R}}$	1.241×10^4	$\frac{\text{meter-newtons}}{\text{meter}^3\text{-degree Kelvin}}$ $\left(\frac{\text{m-N}}{\text{m}^3\text{-}^\circ\text{K}}\right)$
Temperature	degrees Rankine ($^\circ$R)	5/9	degrees Kelvin ($^\circ$K)
Thermal conductivity	$\frac{\text{in-lb}}{\text{in-sec-}^\circ\text{R}}$	8.0068	$\frac{\text{meter-newtons}}{\text{meter-second-degree Kelvin}}$ $\left(\frac{\text{m-N}}{\text{m-sec-}^\circ\text{K}}\right)$
Torque	in-lb	0.11298	meter-newtons (m-N)
Viscosity	centipoises (cP)	0.001	newton-seconds/meter^2 (N-sec/m^2)

*Multiply value given in U.S. Customary Unit by conversion factor to obtain equivalent value in SI Unit.

Prefixes to indicate multiples of units are as follows:

Prefix	Multiple
mega (M)	10^6
centi (c)	10^{-2}
milli (m)	10^{-3}
micro (μ)	10^{-6}

REFERENCES

1. Zener, Clarence: Elasticity and Anelasticity of Metals. Univ. of Chicago Press, c.1948.

2. Granick, Neal; and Stern, Jesse E.: Material Damping of Aluminum by a Resonant-Dwell Technique. NASA TN D-2893, 1965.

3. Baker, W. E.; and Allen, F. J.: The Damping of Transverse Vibrations of Thin Beams in Air. Rept. No. 1033, Ballistic Res. Labs., Aberdeen Proving Ground, Oct. 1957.

4. Stephens, David G.; and Scavullo, Maurice A.: Investigation of Air Damping of Circular and Rectangular Plates, a Cylinder, and a Sphere. NASA TN D-1865, 1965.

5. Osgood, Carl C.: Force Transmissibilities in Spacecraft Structures. Shock Vib. Bull., Bull. 35, Pt. 7, U.S. Dept. Defense, Apr. 1966, pp. 205-211.

6. Ungar, Eric E.: Energy Dissipation at Structural Joints; Mechanisms and Magnitudes. FDL-TDR-64-98, U.S. Air Force, Aug. 1964.

7. Goodman, L. E.; and Klumpp, J. H.: Analysis of Slip Damping With Reference to Turbine-Blade Vibration. J. Applied Mech., vol. 23, no. 3, Sept. 1956, pp. 421-429.

8. Pian, T. H. H.; and Hallowell, F. C., Jr.: Structural Damping in a Simple Built-Up Beam. Proceedings of the First U.S. National Congress of Applied Mechanics, Am. Soc. Mech. Engrs., c.1952, pp. 97-102.

9. Pian, T. H. H.: Structural Damping of a Simple Built-Up Beam With Riveted Joints in Bending. J. Applied Mech., vol. 24, no. 1, Mar. 1957, pp. 35-38.

10. Mentel, T. J.: Vibrational Energy Dissipation at Structural Support Junctions. Structural Damping, Jerome E. Ruzicka, ed., Am. Soc. Mech. Engrs., c.1959, pp. 89-116.

11. Technical Information Staff, Industrial Fasteners Institute: Joint Design. Machine Design, vol. 35, no. 7, Mar. 21, 1963, pp. 29-45.

12. Klint, R. V.; and Owens, R. S.: The Effect of Root Lubrication on the Damping of Cantilever Beams. Trans. Am. Soc. Lubrication Engrs., vol. 3, Apr. 1960, pp. 149-156.

13. Ruzicka, Jerome E.; Derby, Thomas F.; Schubert, Dale W.; and Pepi, Jerome S.: Damping of Structural Composites With Viscoelastic Shear-Damping Mechanisms. NASA CR-742, 1967.

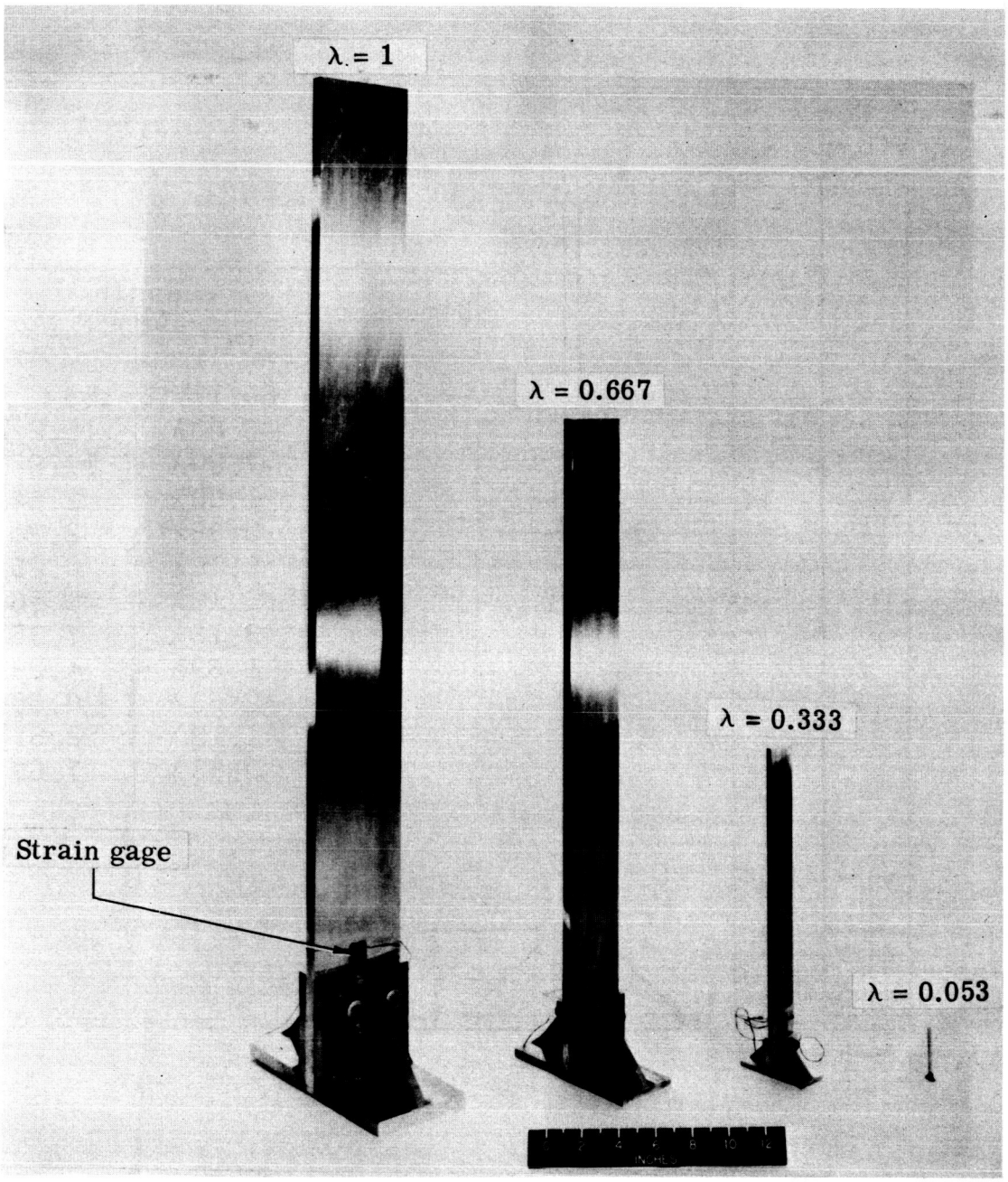

Figure 1.- Photograph illustrating relative sizes of joint damping models. L-67-1054

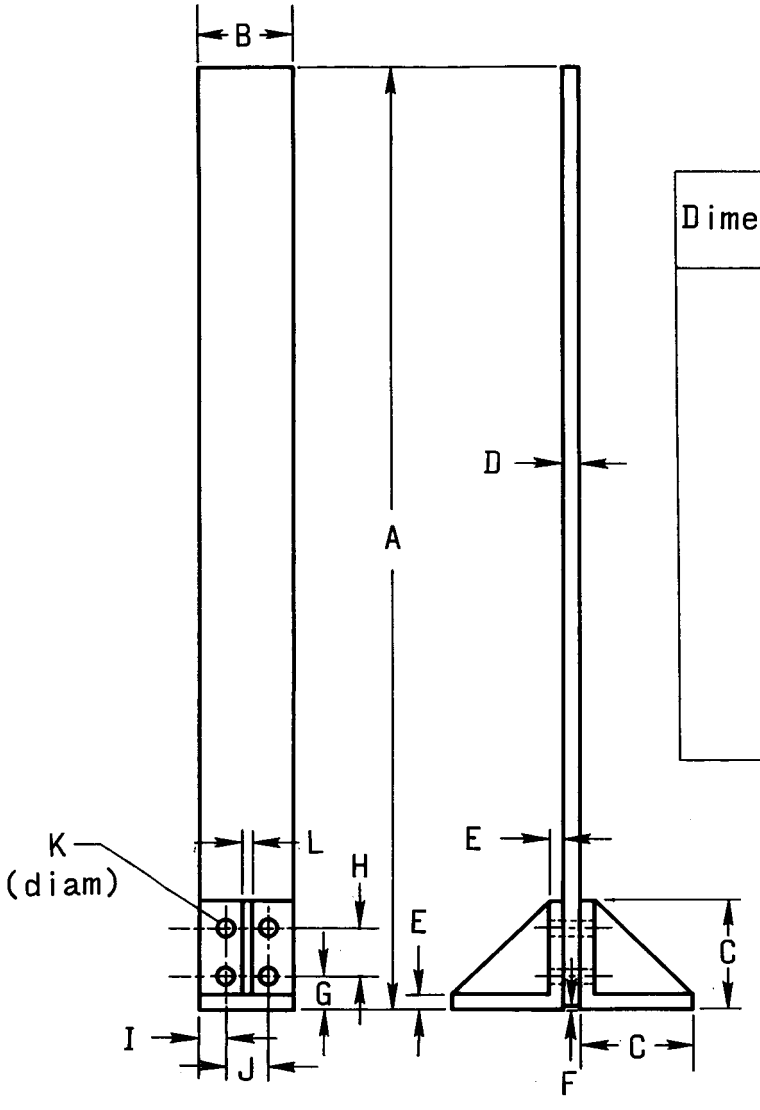

Dimension	Length	
	in.	cm
A	60.1 λ	153 λ
B	6.00λ	15.2 λ
C	7.00λ	17.8 λ
D	1.00λ	2.54λ
E	0.88λ	2.24λ
F	0.10λ	0.25λ
G	2.19λ	5.56λ
H	3.13λ	7.95λ
I	1.69λ	4.29λ
J	2.63λ	6.68λ
K	1.13λ	2.87λ
L	0.63λ	1.60λ

Figure 2.- Dimensions of joint damping models. (Scale factors λ equal to 1, 0.667, 0.333, and 0.053.)

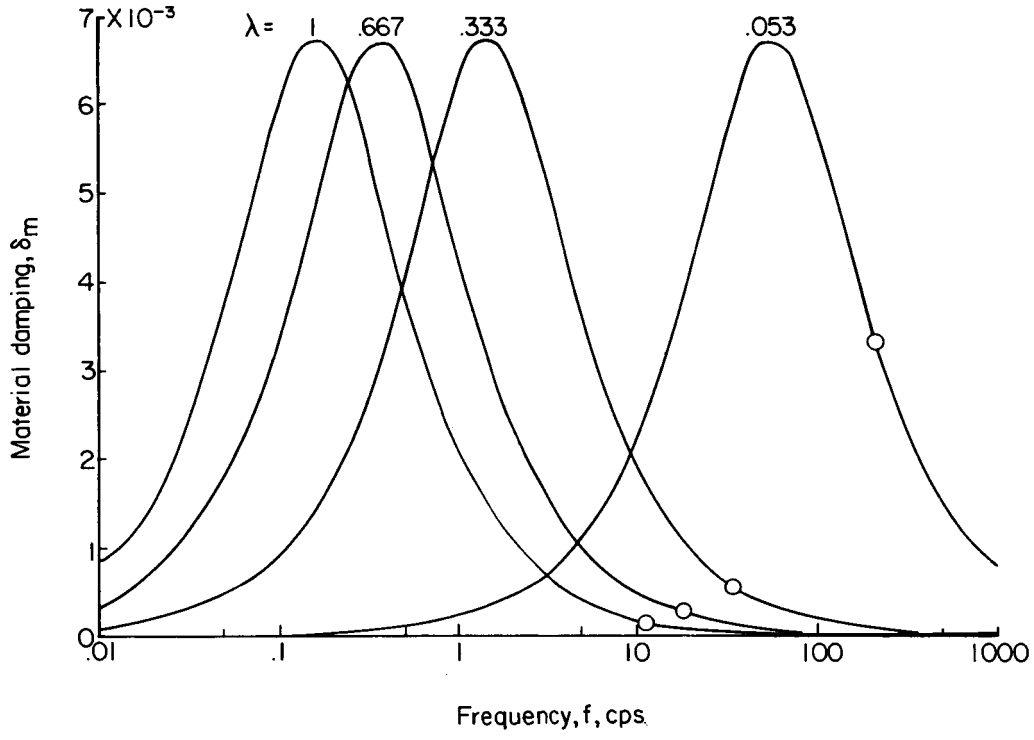

(a) Variation of material damping with frequency.

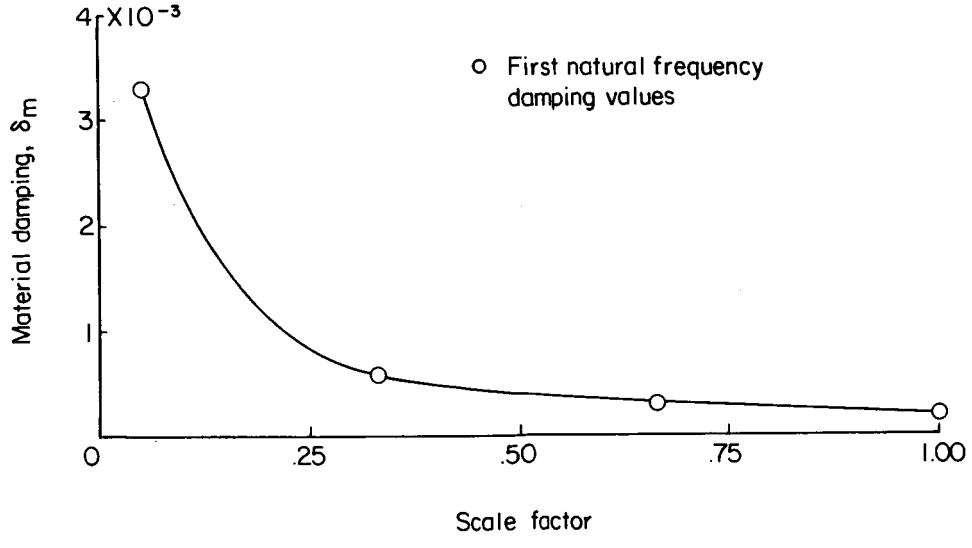

(b) Variation of material damping with scale factor.

Figure 3.- Material damping characteristics of test beams as predicted by relationship of reference 1.

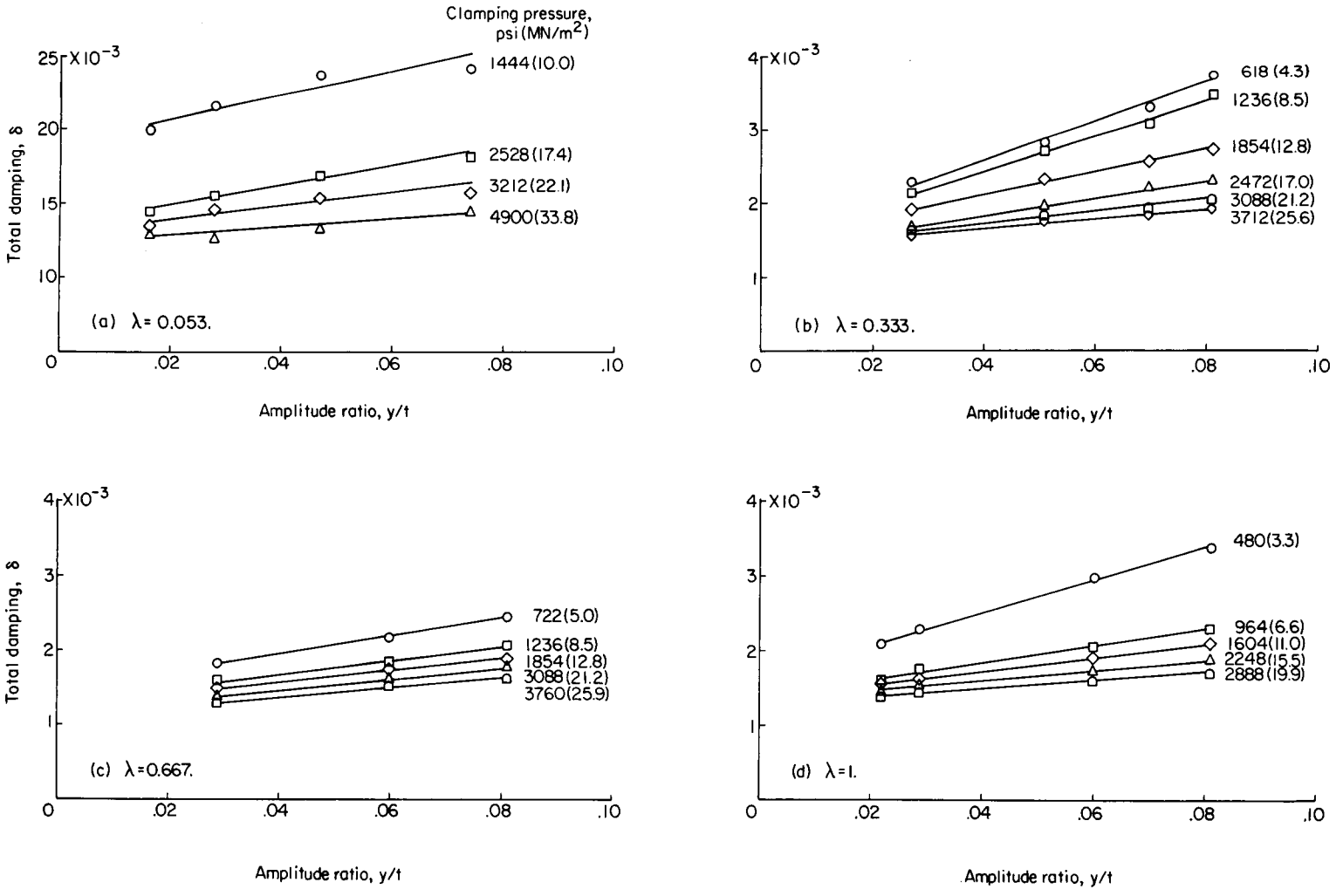

Figure 4.- Variation of total damping with amplitude ratio for a range of joint clamping pressures. Dry joint interfaces.

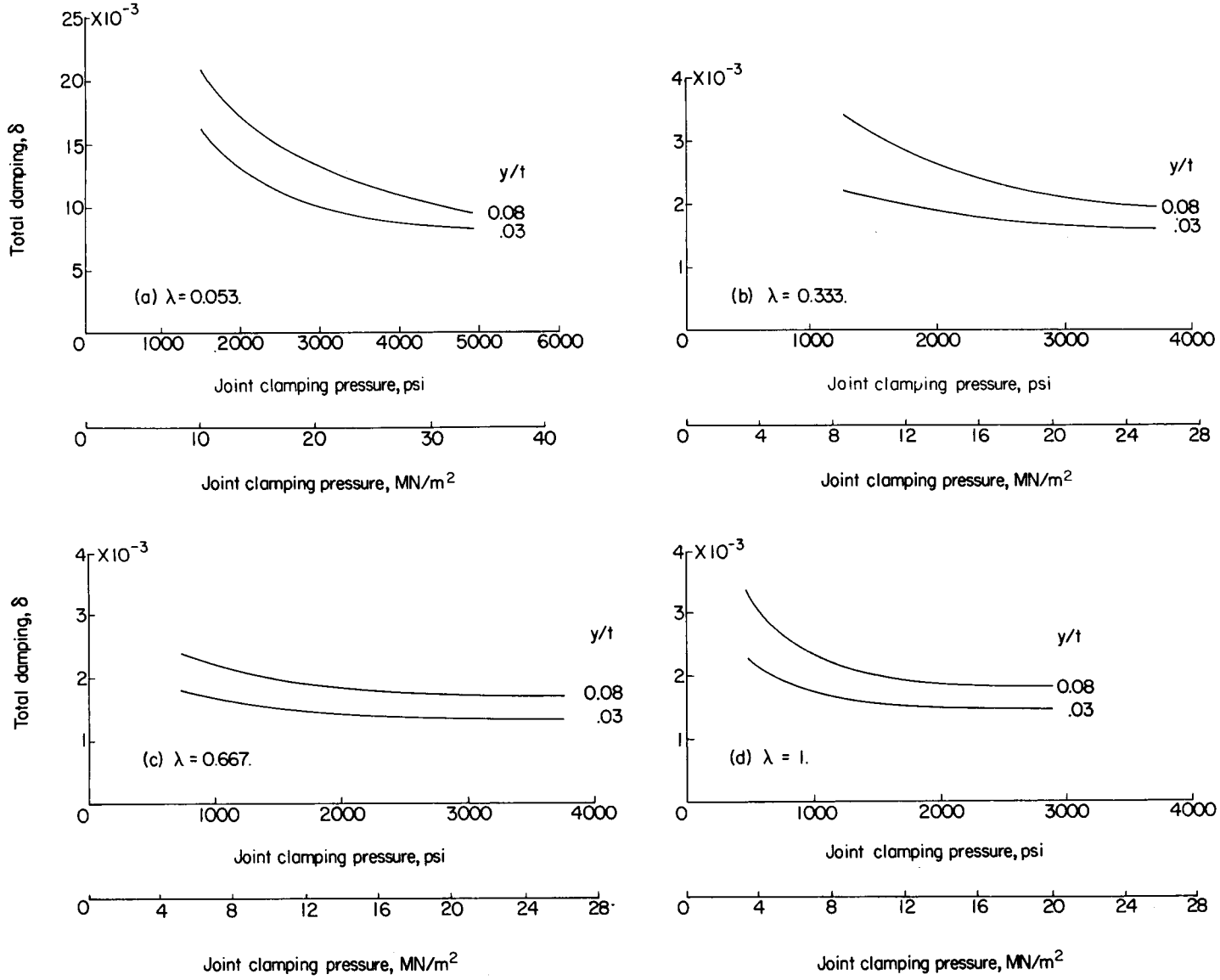

Figure 5.- Variation of total damping with joint clamping pressure. Dry joint interfaces.

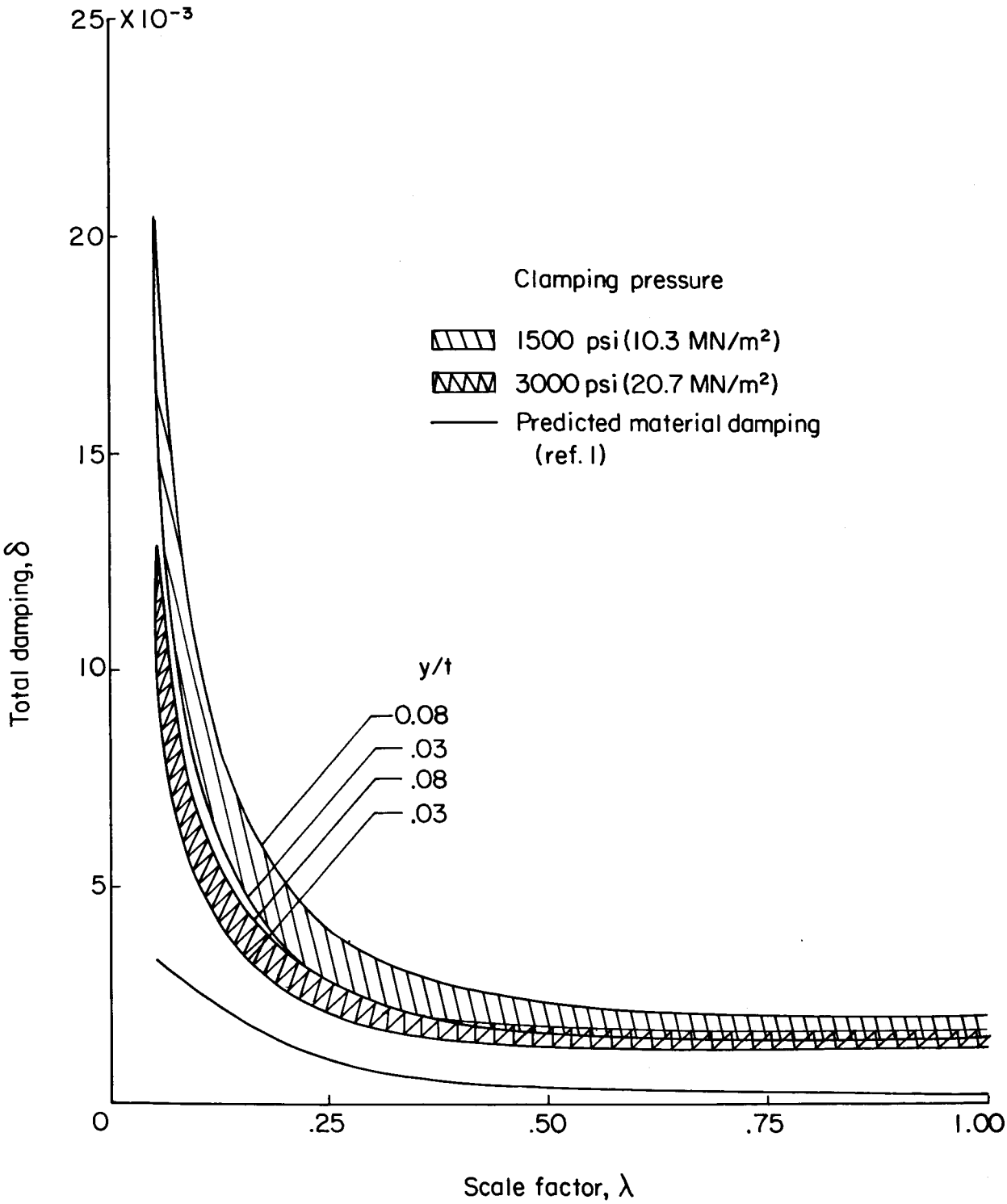

Figure 6.- Variation of total damping with scale factor for a range of amplitude ratios and joint clamping pressures. Dry joint interfaces.

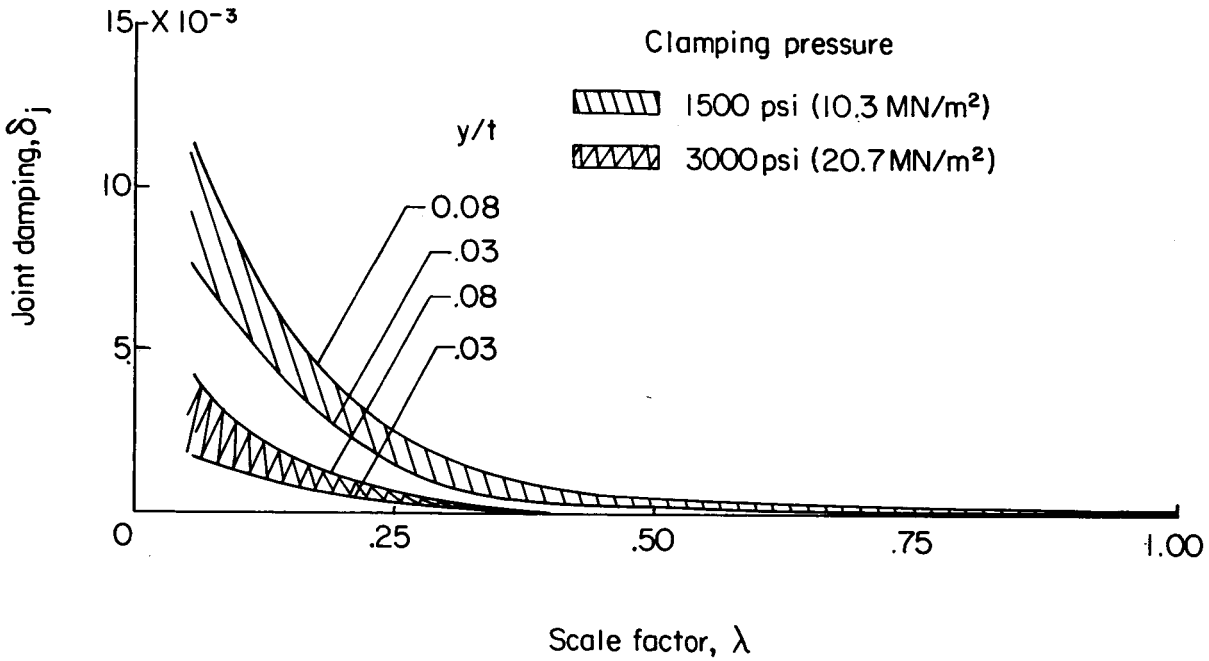

(a) Data for all four beams.

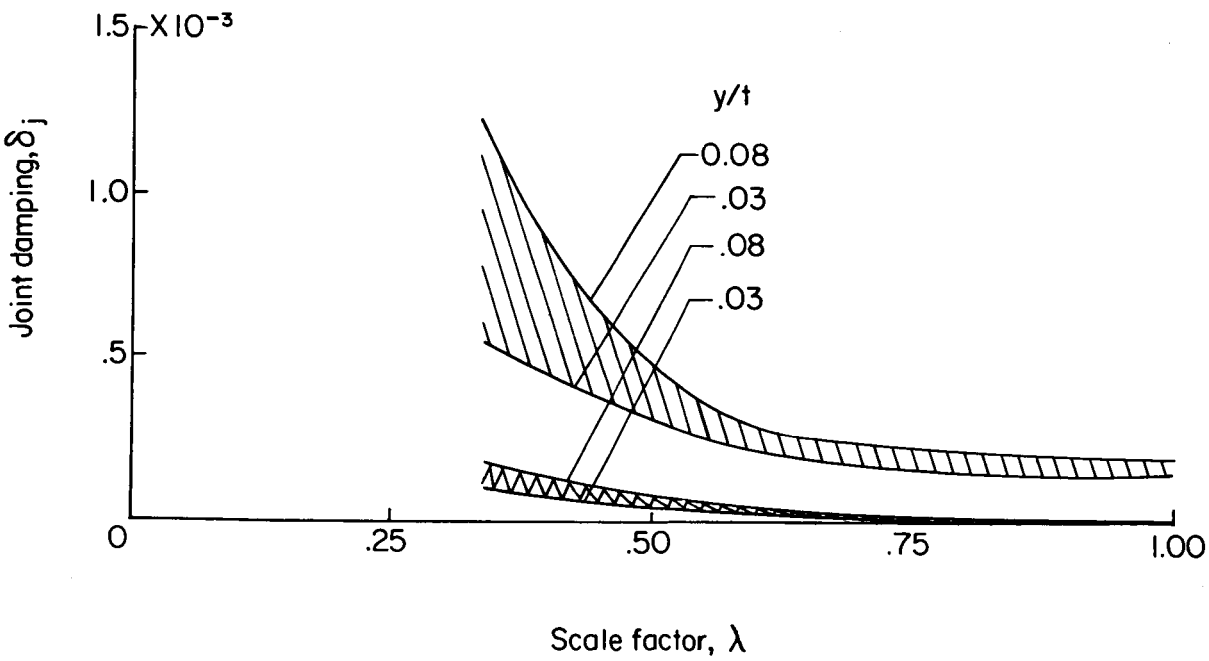

(b) Data for the three larger beams. (Note magnified damping scale.)

Figure 7.- Variation of joint damping with scale factor for a range of amplitude ratios and clamping pressures. Dry joint interfaces.

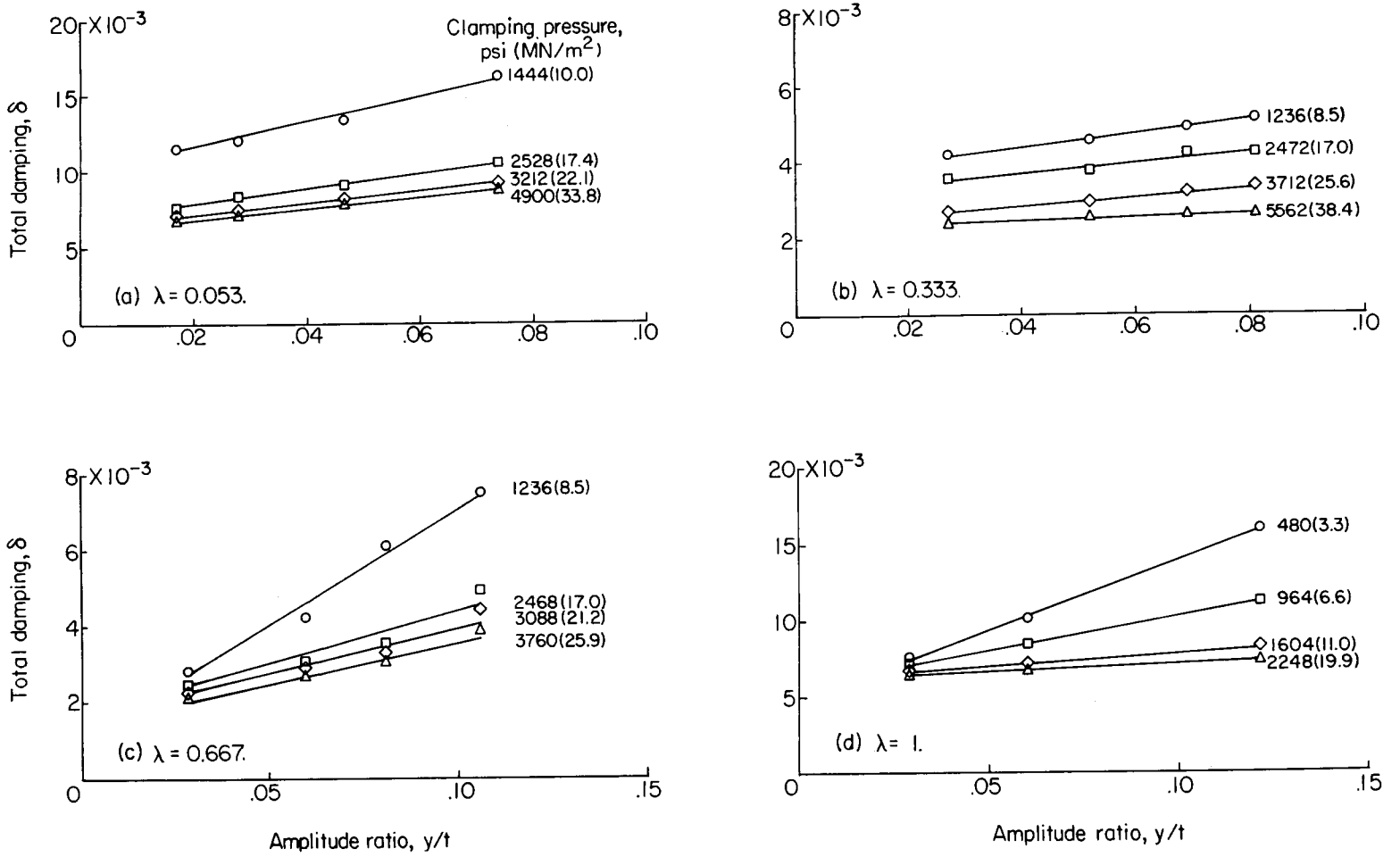

Figure 8.- Variation of total damping with amplitude ratio. Oil-lubricated joint interfaces (μ = 150 cP).

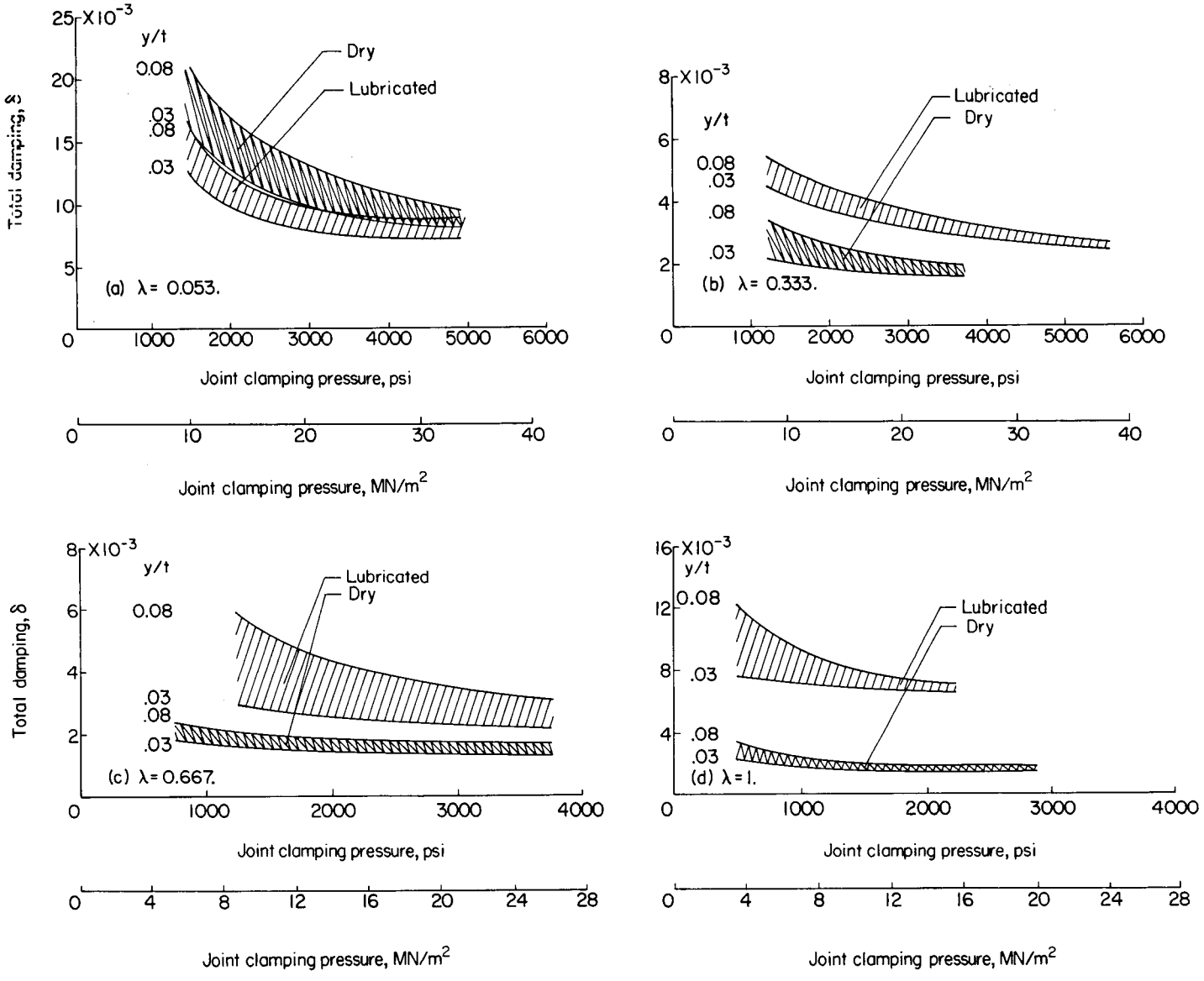

Figure 9.- Variation of total damping with joint clamping pressure for a range of amplitude ratios. Oil-lubricated (μ = 150 cP) and dry joint interface conditions.

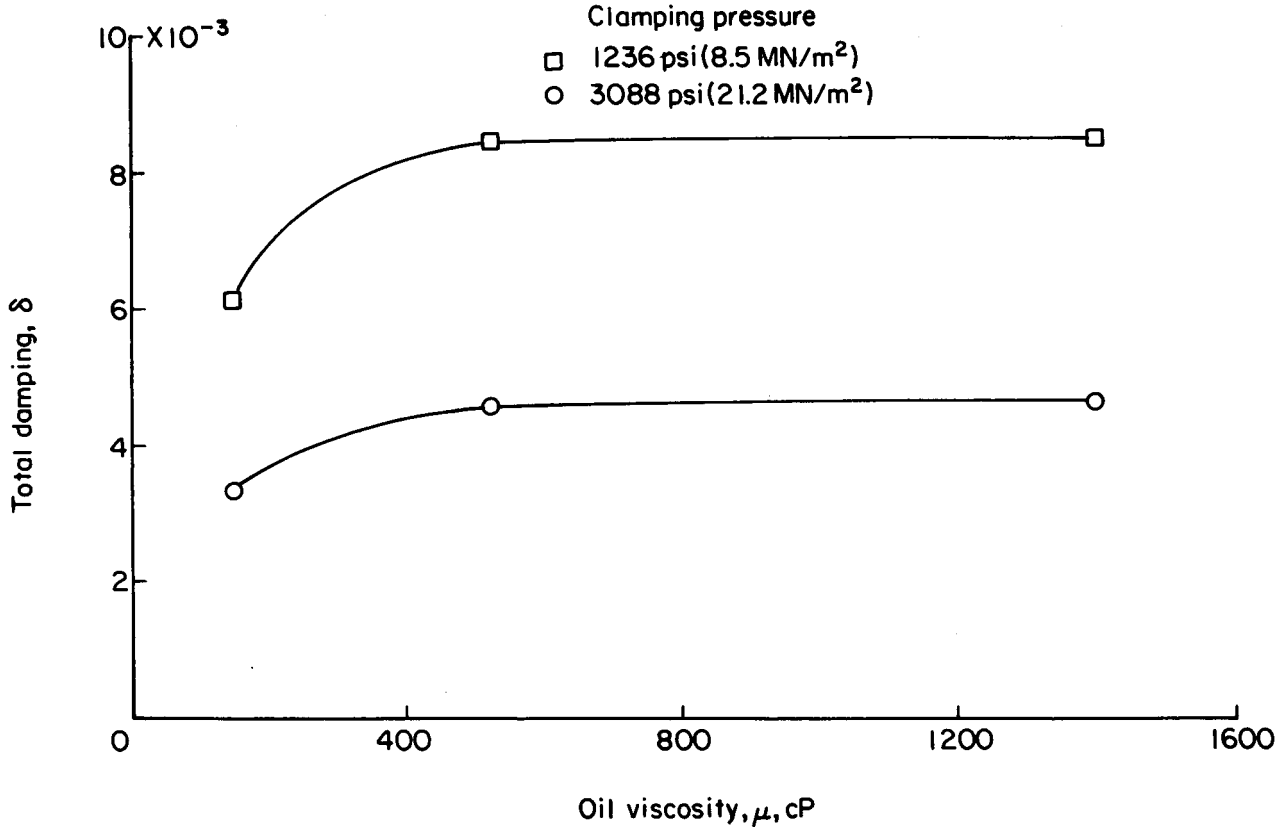

Figure 10.- Variation of total damping with viscosity of joint lubricant. $y/t = 0.08$; $\lambda = 0.667$.

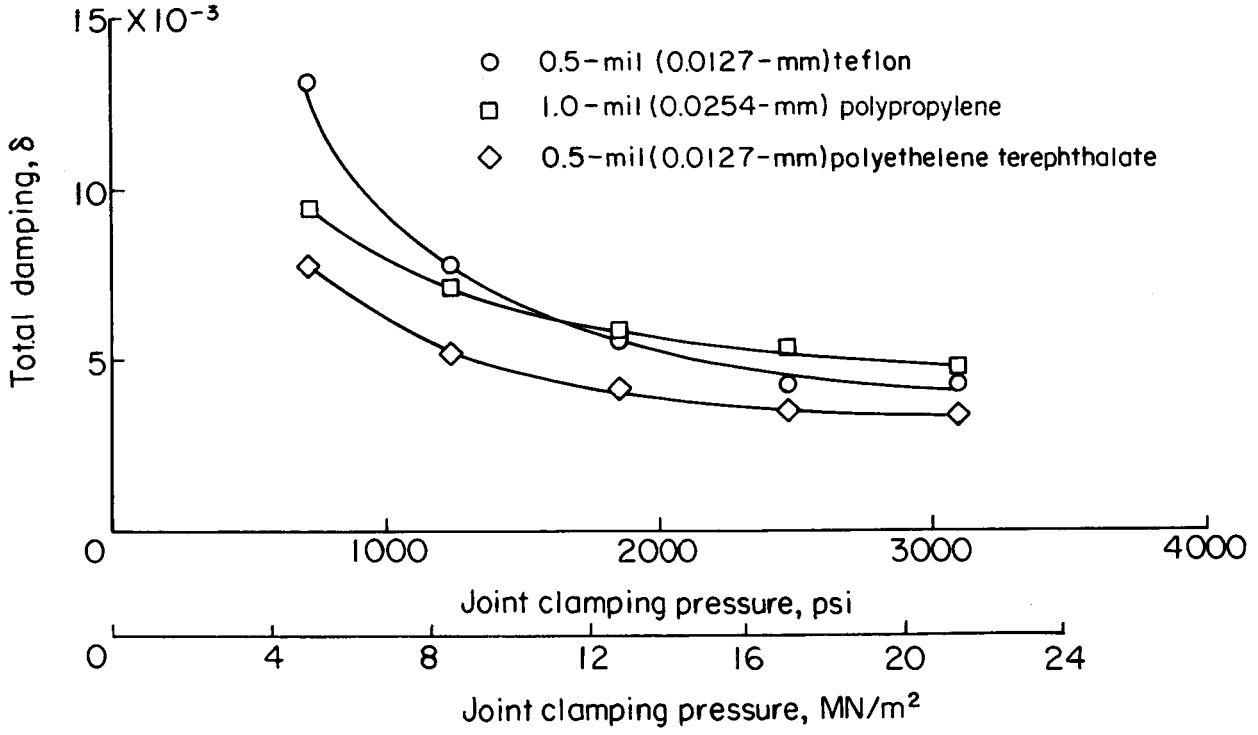

(a) Variation of total damping with joint clamping pressure.

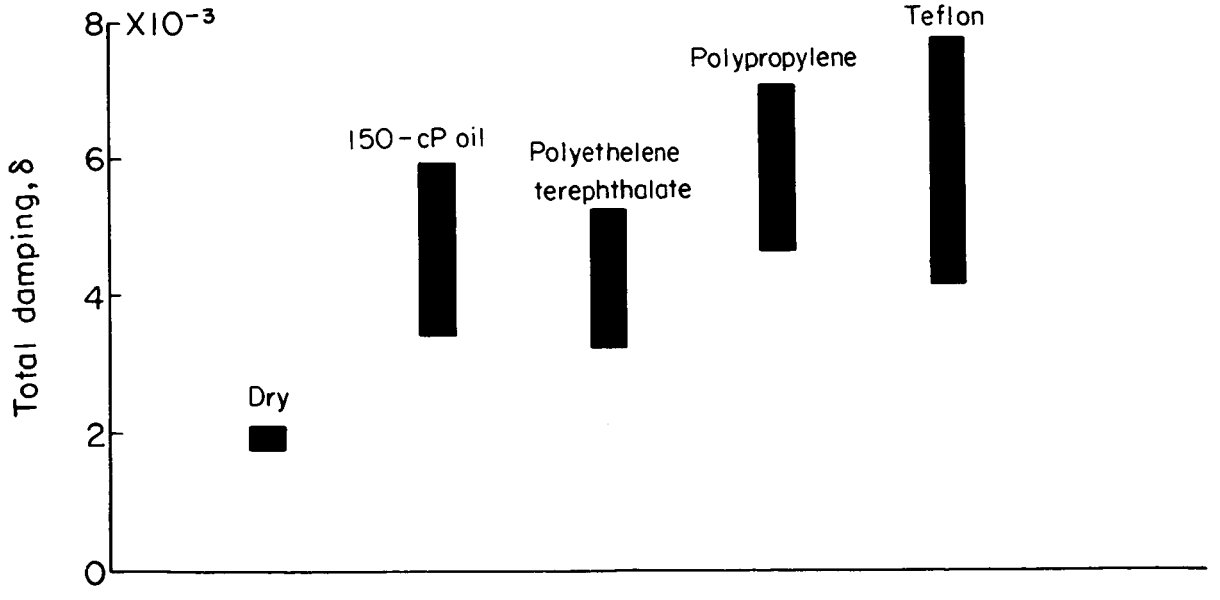

(b) Comparison of total damping for various joint conditions. Length of band indicates damping over 1236 to 3088 psi (8.5 to 21.2 MN/m²) clamping pressure range.

Figure 11.- Effect on damping of adding plastic film inserts to joint interfaces. $\lambda = 0.667$; $y/t = 0.08$.